

CHROM. 19 413

THREE-DIMENSIONAL NETWORK PLOTS IN SUPERCRITICAL FLUID CHROMATOGRAPHY WITH *n*-PENTANE-1,4-DIOXANE

DAGMAR LEYENDECKER, FRANZ P. SCHMITZ*, DIETGER LEYENDECKER and ERNST KLESPEL

Lehrstuhl für Makromolekulare Chemie, RWTH Aachen, Worringerweg, D-5100 Aachen (F.R.G.)

(Received January 12th, 1987)

SUMMARY

Using *n*-pentane-1,4-dioxane as a binary eluent system in supercritical fluid chromatography (SFC) and silica as the stationary phase, three-dimensional network plots of capacity ratios, k' , selectivities, α , effective plate numbers, N , and resolutions, R , of four polycyclic aromatic hydrocarbons *versus* column temperature and eluent composition at constant column pressure were obtained. Although the effects of the physical parameters temperature, composition and pressure on the chromatographic properties k' , α , N or R of the binary eluent are found to be complex in detail, general information can be derived from the three-dimensional plots. The individual shapes of all three-dimensional surfaces are similar inasmuch as they are characterized by elevations located above the boiling temperature, T_b , when the pressure is subcritical, or above the critical temperature, T_c , at supercritical pressures of the eluent mixtures. Differences exist between k' , α , N and R with respect to the individual shapes and details of the elevations. Whereas above T_b or T_c the selectivities, α , for instance, remain high relatively independent of composition, the other chromatographic parameters change considerably with composition. An increase in pressure always reduces the overall height of the elevations.

INTRODUCTION

In supercritical fluid chromatography (SFC), it can be advantageous to use binary mobile phases instead of pure eluents. Both the separation speed and the resolution may be improved. The dependence of the chromatographic parameters capacity ratio, k' , selectivity, α , effective plate number, N , and resolution, R , on temperature and pressure is basically similar to that of pure eluents¹⁻³. However, for binary eluents, the dependence on composition also has to be considered, and this dependence is found to be more varied in detail. While two-dimensional graphs give an adequate quantitative representation of the experimental data, a visual overview is more easily obtained with a three-dimensional plot which is drawn to different perspectives, if needed⁴.

Based on an earlier investigation on the binary mobile phase pentane-1,4-diox-

ane, silica gel as the stationary phase and the four polycyclic aromatic hydrocarbons naphthalene, anthracene, pyrene and chrysene as the substrate⁵, this work offers additional data including those on α and N . In the three-dimensional graphs presented, one of the chromatographic parameters, k' , α , N or R , is plotted on the third axis, with temperature and eluent composition on the remaining two. Although the graphs are isobaric, a comparison of two graphs obtained at different pressures indicates, of course, the influence of pressure. The chromatographic parameter that was not varied was the volume feed rate of the mobile phase. Thus, all data have been obtained with a constant feed rate for the liquid binary eluent mixture. The isobaric networks demonstrate considerable complexity of the interrelations, and also several basic features that are useful for the optimization of separations with varying temperature, composition and/or pressure.

EXPERIMENTAL

The chromatograms were run on an SFC instrument constructed from commercially available high-performance liquid chromatographic (HPLC) components, as described previously⁴. The volume flow-rate of the liquid mobile phase, as measured at the pumps at ambient temperature, was kept at 1 ml/min. Detection was effected in the liquid state at ambient temperature with a variable-wavelength UV detector at 254 nm. Stainless-steel columns (25 cm \times 4.6 mm I.D.) were packed with LiChrosorb Si 100, 10 μ m (Merck, Darmstadt, F.R.G.) using a slurry method. *n*-Pentane, 1,4-dioxane and *n*-heptane (for measuring the dead time) were dried over sodium and distilled. 1,4-Dioxane had to be distilled twice to obtain a sufficient purity. *n*-Pentane and 1,4-dioxane were pre-mixed before the isothermal-isobaric-isocratic chromatographic runs and metered as a mixture.

The chromatographic parameters k' , α , N , R^* and R_m were calculated by use of the following equations:

Capacity ratio:

$$k' = \frac{t_R - t_0}{t_0} \quad (1)$$

Selectivity between two peaks i and j :

$$\alpha_{i,j} = \frac{k'_j}{k'_i} = \frac{t_{R,j} - t_0}{t_{R,i} - t_0} \quad (2)$$

Effective plate number:

$$N = \left(\frac{t_R - t_0}{w'} \right)^2 \cdot 8 \ln 2 \quad (3)$$

Resolution between two peaks i and j ⁶:

$$R_{i,j}^* = \frac{f_{i,j}}{g_{i,j}} + \frac{d_{i,j}}{w'_i + w'_j} \cdot \sqrt{\ln 4} \quad (4)$$

Mean resolution:

$$R_m = \frac{\sum_{i,j}^n R_{i,j}^*}{n} \quad (5)$$

where t_R is the retention time, t_0 the dead time, $f_{i,j}$ the depth of the valley between two neighbouring peaks, $g_{i,j}$ their average peak height, $d_{i,j}$ the distance between the baseline intercepts of the inner tangents to the two neighbouring peaks and w' their width at half-height.

RESULTS AND DISCUSSION

Series of isothermal–isobaric–isocratic chromatographic runs were performed. First, the temperature was varied between runs, then the eluent composition and finally the pressure. Thus, at a constant pressure at the column outlet, p_e , chromatographic runs were carried out with ten different eluent compositions from 100% *n*-pentane up to 100% 1,4-dioxane. For each composition, the temperature was varied in eight steps from 25 to 300°C. The resulting combinations of temperature and eluent composition for 80 chromatograms are shown in the two-dimensional net in Fig. 1 as points where two lines meet. The parameters k' , α , N and R_m were calculated from

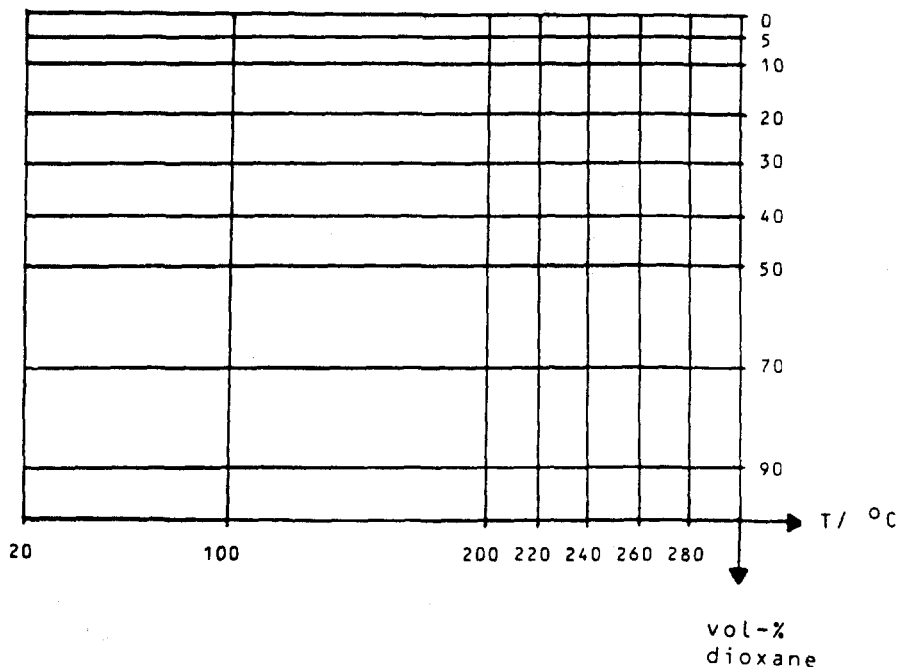


Fig. 1. Temperatures, T , and column end pressure, p_e , employed for 80 chromatographic runs, as represented by a net.

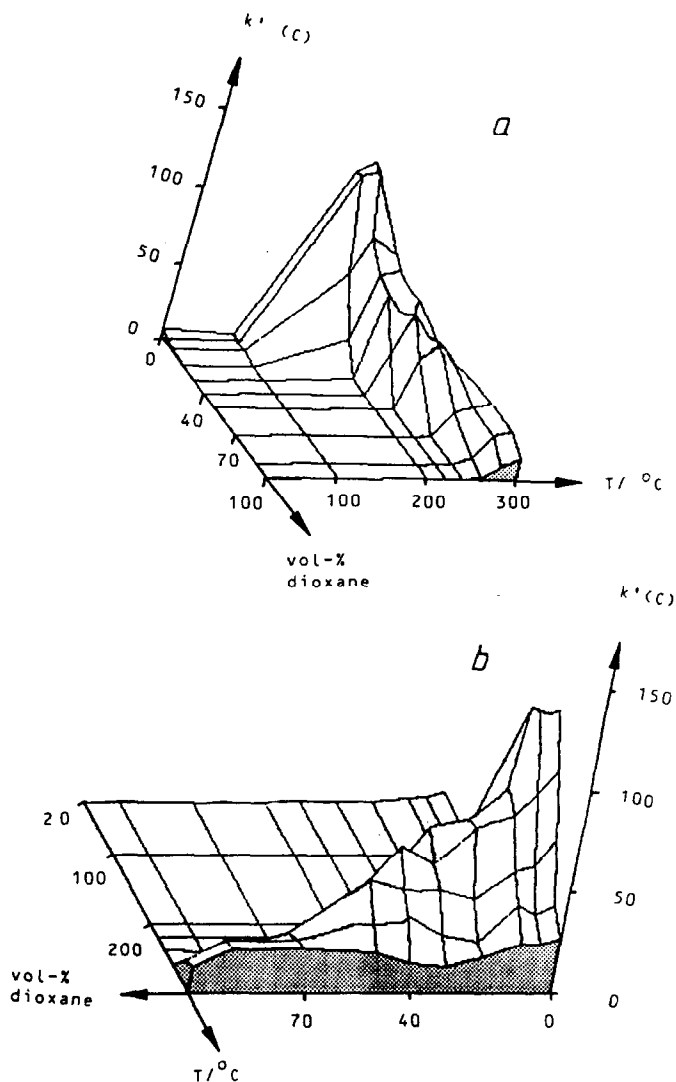


Fig. 2. Dependence of the capacity ratio of chrysenes, $k'(C)$, on temperature, T , and eluent composition, vol.-% 1,4-dioxane, in two perspectives, a and b. Column outlet pressure, $p_c = 20$ bar.

each chromatogram and one of them plotted as the z-axis, with composition and temperature being the x- and y-axes, respectively. For the actual drawing of the three-dimensional isobaric nets a computer program was used⁷.

In Figs. 2-4, the k' values for chrysenes, $k'(C)$, and anthracene, $k'(A)$, are shown as a function of temperature and composition. For the graph of $k'(C)$ in Fig. 2 two different perspectives, a and b, are given. A prominent feature of the graph is an elevation that is situated in the gaseous region above the boiling temperature. The elevation can be described as a "mountain ridge" that slopes downwards and moves

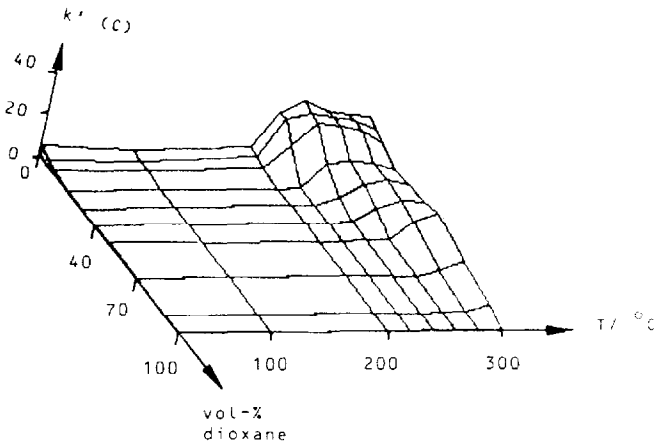


Fig. 3. Dependence of capacity ratio of chrysene, $k'(C)$, on temperature, T , and eluent composition; $p_e = 36$ bar.

simultaneously to higher temperature when the amount of 1,4-dioxane is increased. While a view of the "mountain ridge", as seen from lower temperature, is given by perspective a, the other side of the elevation can be inspected by perspective b. Increasing the 1,4-dioxane content from 0 to 5% has little effect, but increasing it further results in a substantial decrease. This decrease may, however, be reversed at certain 1,4-dioxane contents to yield a small intermediate rise in k' . In such a range of 1,4-dioxane contents, an increase in 1,4-dioxane leads to an increase in k' instead of the usual decrease.

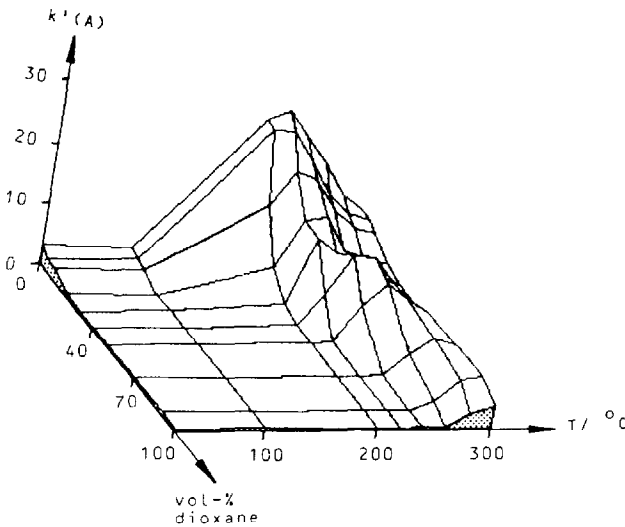


Fig. 4. Dependence of the capacity ratio of anthracene, $k'(A)$, on temperature, T , and eluent composition; $p_e = 20$ bar.

The effect of pressure on $k'(C)$ can be derived from Fig. 3, which corresponds to the same perspective as Fig. 2a. The higher pressure of 36 bar in Fig. 3, as opposed to 20 bar in Fig. 2, leads to a much lower elevation. The k' values of the other three polycyclic aromatic hydrocarbons have a similar three-dimensional surface. This is demonstrated by the capacity ratio of anthracene, $k'(A)$, at 20 bar in Fig. 4. Comparison with Fig. 2 shows that eluents of lower molecular size lead to lower elevations.

The behaviour of the selectivity, α , in Figs. 5–8 is different from that of k' , inasmuch as the observed elevations tend to have more the appearance of a “high plateau” than of a well developed “mountain ridge”, the latter sloping down instantly to both lower and higher temperatures. The “plateau” in some instances is clefted and has smaller peaks on its surface. In this connection it should be noted that the isobaric three-dimensional surface is defined by relatively few intersections (and tees),

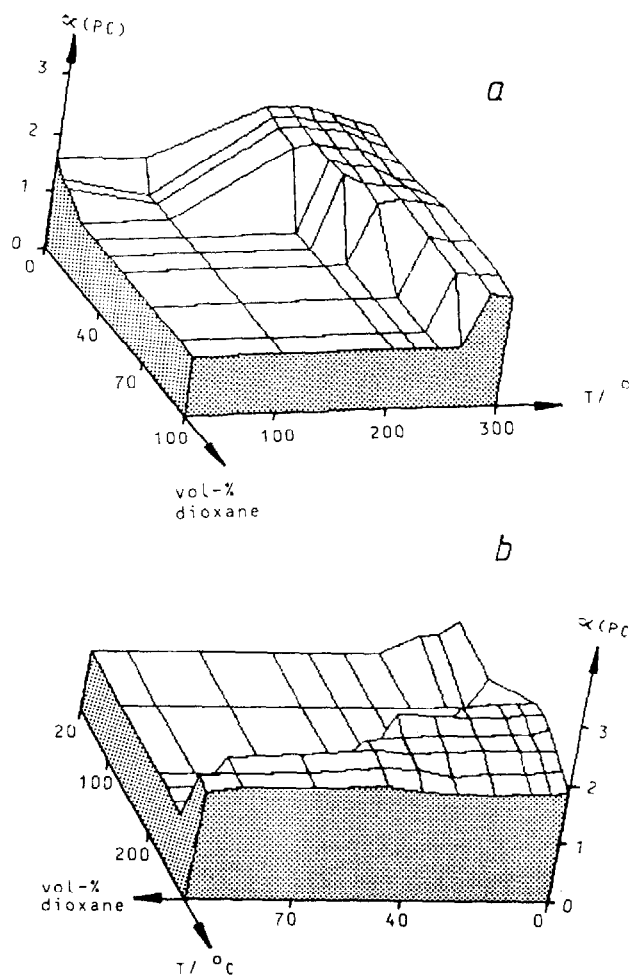


Fig. 5. Dependence of the selectivity, α , between pyrene and chrysene, $\alpha(PC)$, on temperature, T , and eluent composition, vol.-% 1,4-dioxane, in two perspectives, a and b. Column outlet pressure, $p_e = 20$ bar.

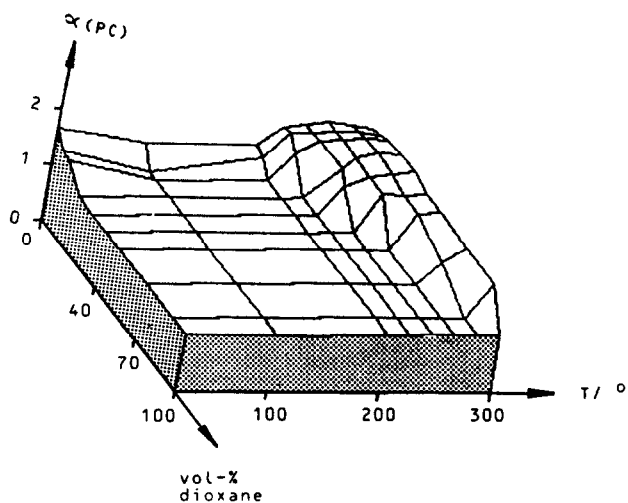


Fig. 6. Dependence of the selectivity between pyrene and chrysene, $\alpha(PC)$, on temperature, T , and eluent composition; $p_e = 36$ bar.

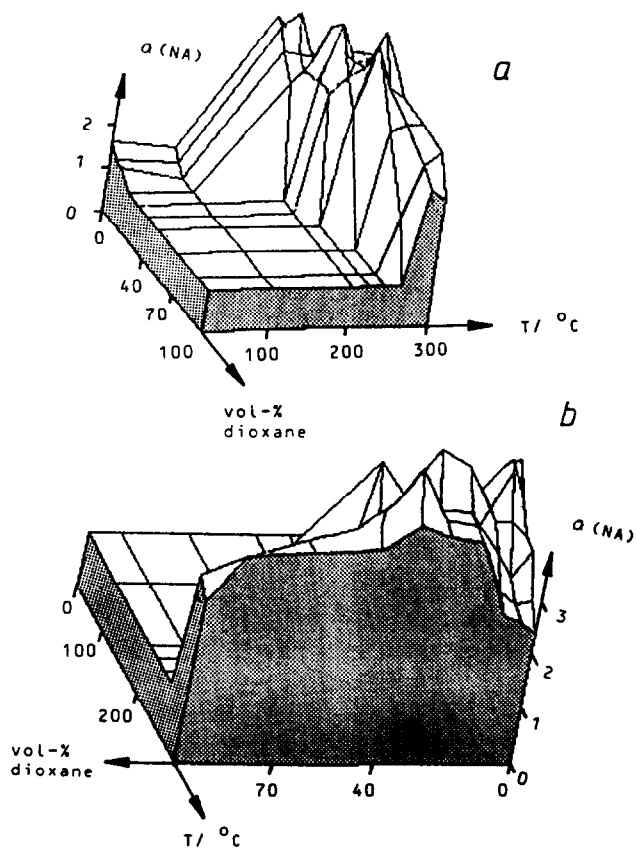


Fig. 7. Dependence of the selectivity between naphthalene and anthracene, $\alpha(NA)$, on temperature, T , and eluent composition in two perspectives, a and b; $p_e = 20$ bar.

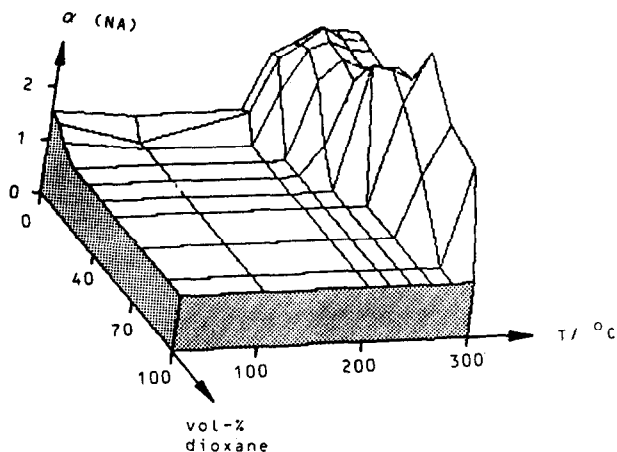


Fig. 8. Dependence of the selectivity between naphthalene and anthracene, $\alpha(NA)$, on temperature, T , and eluent composition; $p_e = 36$ bar.

which makes the accurate location and height of these smaller peaks uncertain. In Figs. 5–8 the α values are shown for two of the three pairs of neighbouring peaks. Starting with the selectivity between the two largest elutes, pyrene and chrysene, $\alpha(PC)$, in Figs. 5 and 6, a higher 1,4-dioxane content does not substantially decrease α , as was the case with k' . However, a higher pressure reduces α considerably, in keeping with the behaviour of k' . The selectivities between the two smallest elutes, naphthalene and anthracene, $\alpha(NA)$, in Figs. 7 and 8 show a similar behaviour to $\alpha(PC)$, with respect to both the effect of the 1,4-dioxane content and the effect of pressure.

The graphs for the effective plate numbers, N , are shown in Figs. 9–12. The N values show a particularly clefted appearance with more than one larger peak in the gaseous state. Remarkable is also the substantial elevation in the liquid state at very low 1,4-dioxane contents. The effective plate numbers for chrysene, $N(C)$, are given in Figs. 9 and 10 at 20 and 36 bar, respectively. A rapid overall fall of N is observable with increasing 1,4-dioxane content, and there is also an overall decrease in N with increasing pressure. These observations also apply to the effective plate numbers of anthracene, $N(A)$, in Figs. 11 and 12.

The parameters α and N contribute to the resolution R according to the equation

$$R_{i,j} = \frac{1}{4} \cdot \frac{\alpha_{i,j} - 1}{\alpha_{i,j}} \cdot \sqrt{N_j} \quad (6)$$

Because both α and N show large elevations in the three-dimensional isobaric surfaces, at a temperature which is either above boiling (at subcritical pressures) or above the critical temperature (at supercritical pressures), it is to be expected that the same will occur for $R_{i,j}^*$ and R_m . Figs. 13 and 14 show the elevations for R_m at 20 and 36 bar, respectively. Again, there is a clefted appearance of the elevations. They

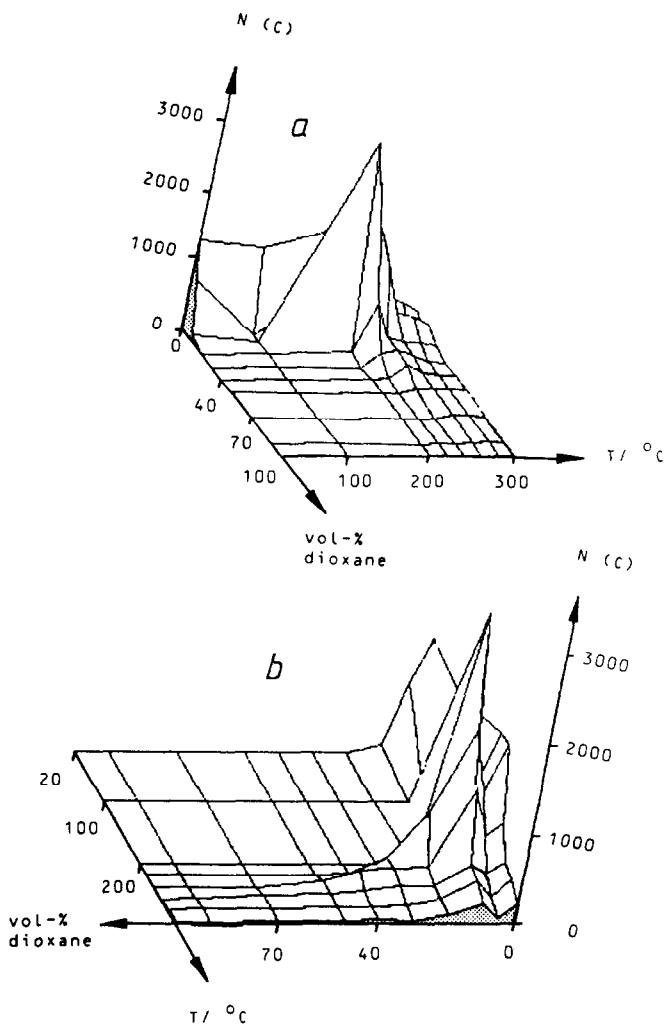


Fig. 9. Dependence of the effective plate number of chrysene, $N(C)$, on temperature, T , and eluent composition in two perspectives, a and b; $p_c = 20$ bar.

also decrease in height and move to higher temperatures both with increasing 1,4-dioxane content and with increasing pressure. At low 1,4-dioxane contents the changes in $\sqrt{N_j}$ are larger than those in $(\alpha_{i,j} - 1)/\alpha_{i,j}$. This term is then decisive for the changes in $R'_{i,j}$ and R_m . At higher 1,4-dioxane contents, however, the term $(\alpha_{i,j} - 1)/\alpha_{i,j}$ becomes more important.

Perspective three-dimensional graphs like those in Figs. 2–14 are not suitable for reading off chromatographic parameters quantitatively. For this purpose, series of parallel cross-sections of these graphs can be utilized, *i.e.*, cuts parallel to the z -axis (k' , α , N , R_m) and parallel to either the y -axis (temperature) or the x -axis (eluent composition). Such cross-sections (projections) have been shown previously, using

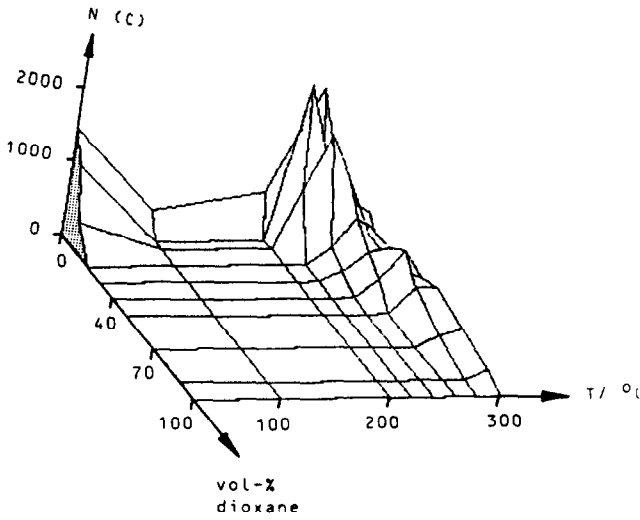


Fig. 10. Dependence of the effective plate number of chrysene, $N(C)$, on temperature, T , and eluent composition; $p_e = 36$ bar.

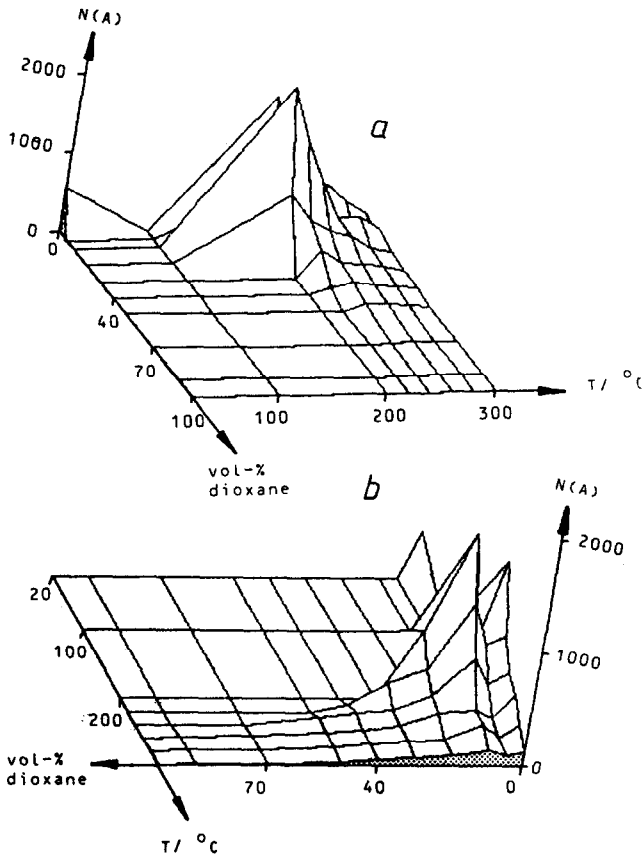


Fig. 11. Dependence of the effective plate number of anthracene, $N(A)$, on temperature, T , and eluent composition in two perspectives, a and b; $p_e = 20$ bar.

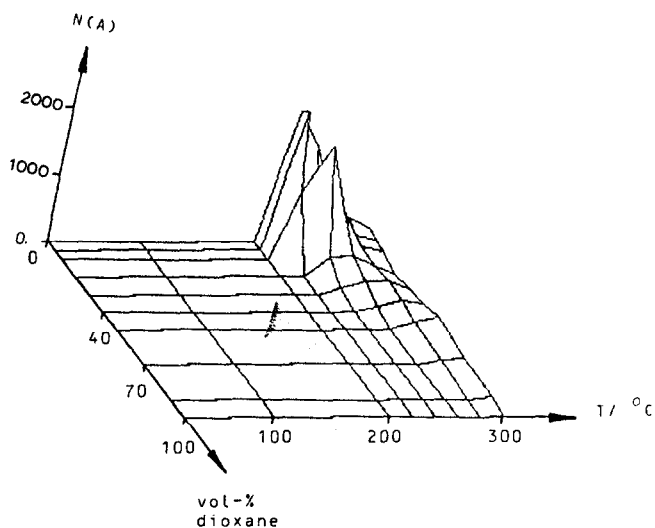


Fig. 12. Dependence of the effective plate numbers of anthracene, $N(A)$, on temperature, T , and eluent composition; $p_e = 36$ bar.

data obtained for the same mobile phase, stationary phase and substrate⁵. The projections always showed maxima of k' or R_m versus temperature, as they obviously must on inspecting the three-dimensional graphs. Maxima were also found in some instances when k' or R_m was plotted versus eluent composition. This is also in accord with the three-dimensional graphs, as the elevations often have a maximum in a given isothermal contour. These maxima have been explained by a preferential adsorption

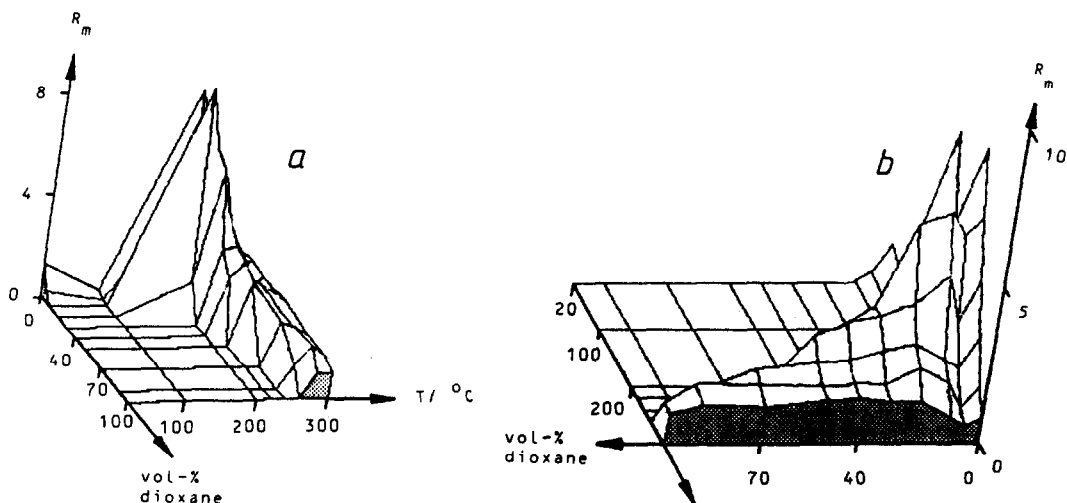


Fig. 13. Dependence of the mean resolution, R_m , on temperature, T , and eluent composition in two perspectives, a and b; $p_e = 20$ bar.

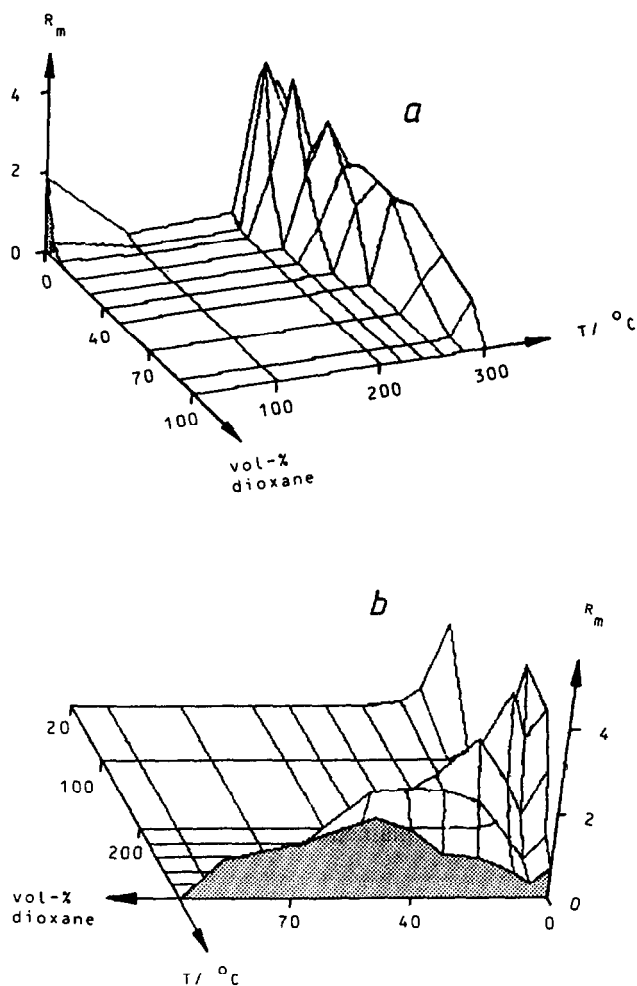


Fig. 14. Dependence of the mean resolution, R_m , on temperature, T , and eluent composition in two perspectives, a and b; $p_e = 36$ bar.

of the 1,4-dioxane on the silica stationary phase which is dependent on the percentage by volume of 1,4-dioxane in the mobile phase⁵. Such maxima, however, do not necessarily lead to the clefted appearance that is seen particularly for the elevations of the three-dimensional plots for α , N and R_m . A clefted appearance may arise whenever the chromatographic parameters are composed of more than one variable. For instance, α is given by k'_j and k'_i , as defined by eqn. 2. The k' values may have different slopes and reach their maxima at different temperatures⁵, thereby leading to a complicated behaviour of α .

The three-dimensional graphs shown here pertain either to a subcritical pressure of 20 bar or to a pressure of 36 bar, the latter being subcritical over part of the range of composition ($p_c = 33.7$ bar for pure *n*-pentane). Experiments showed, how-

ever, that similar results may also be obtained at moderate supercritical pressures up to 70 bar. However, with higher pressures the height of the elevations decreases.

ACKNOWLEDGEMENTS

Thanks are expressed to Mr. B. Lorenschat for technical aid and to the Arbeitsgemeinschaft Industrieller Forschungsvereinigungen for financial support.

REFERENCES

- 1 D. Leyendecker, F. P. Schmitz and E. Klesper, *J. Chromatogr.*, 315 (1984) 19.
- 2 D. Leyendecker, F. P. Schmitz, D. Leyendecker and E. Klesper, *J. Chromatogr.*, 321 (1985) 273.
- 3 D. Leyendecker, D. Leyendecker, F. P. Schmitz and E. Klesper, *J. Chromatogr.*, 371 (1986) 93.
- 4 D. Leyendecker, D. Leyendecker, F. P. Schmitz and E. Klesper, *J. High Resolut. Chromatogr. Chromatogr. Commun.*, 9 (1986) 566.
- 5 D. Leyendecker, D. Leyendecker, F. P. Schmitz and E. Klesper, *J. Chromatogr.*, 392 (1987) 101.
- 6 F. P. Schmitz, *J. Chromatogr.*, 356 (1986) 261.
- 7 O. Guenter, in *64'er*, Sonderheft 4/85, Verlag Markt & Technik, Haar, 1985, p. 89.